

## A GOES Thermal-Based Drought Early Warning Index for NIDIS

Christopher R. Hain<sup>1</sup>, Martha C. Anderson<sup>2</sup>, Xiwu Zhan<sup>3</sup>, Mark Svoboda<sup>4</sup>, Brian Wardlow<sup>4</sup>,  
Kingtse Mo<sup>5</sup>, John R. Meckalski<sup>6</sup>, William P. Kustas<sup>2</sup>, and Jesslyn Brown<sup>7</sup>

<sup>1</sup>*Earth System Science Interdisciplinary Center, University of Maryland, College Park, MD*

<sup>2</sup>*USDA-ARS Hydrology and Remote Sensing Lab, Beltsville, MD*

<sup>3</sup>*National Drought Mitigation Center, University of NE-Lincoln, Lincoln, NE*

<sup>4</sup>*NESDIS, NOAA, Camp Springs, MD*

<sup>5</sup>*NCEP Climate Prediction Center, Camp Springs, MD*

<sup>6</sup>*University of Alabama in Huntsville, Huntsville, AL*

<sup>7</sup>*USGS Earth Resources Observations and Science (EROS) Center, Sioux Falls, SD*

### 1. Introduction

The interpretation of drought signals has proven to be difficult because of a general lack of ground-based “truth” metrics available at continental scales; therefore, forecasters must rely on a convergence of evidence strategy using multiple drought index datasets. Standard indicators currently used in drought monitoring focus on different components of the water budget: precipitation, soil moisture, groundwater, runoff and streamflow. The goal of our NOAA CPO-funded project is to develop a thermal-based drought index based on estimates of the actual to potential evapotranspiration ratio provided by the Atmosphere Land-Exchange Inverse (ALEXI) model (Anderson, *et al.*, 2007a,b; 2011), focusing on the water-use component of the hydrologic cycle.

Current drought indices include precipitation-based analyses (*e.g.*, Standardized Precipitation Index (SPI; McKee *et al.* 1995); the Palmer indices (Palmer 1965)), and satellite-based vegetation/TIR indices (*e.g.*, Vegetation Health Index (VHI; Kogan 1997); VegDRI (Brown *et al.* 2008)), along with soil moisture and ET datasets generated with land-surface models (LSMs) in the National Land Data Assimilation System (NLDAS; Mitchell *et al.* 2003). Each of these index classes has issues: datasets like NLDAS and SPI require precipitation and/or soil texture fields that are difficult to observe/specify accurately over large spatial domains; while empirical TIR-based drought indices currently in use (like the VHI) do not account for important forcings on land-surface temperature (LST) (*e.g.*, available energy, atmospheric demand), and can therefore generate spurious drought detections under certain circumstances – particularly at high latitudes (Karnieli *et al.* 2006; Karnieli *et al.* 2010).

In contrast, diagnostic LSMs based on TIR remote sensing of LST, like ALEXI, require no information regarding antecedent precipitation or soil moisture storage capacity - *the current surface moisture status is deduced directly from the remotely sensed radiometric temperature signal*. This results in a seamless implementation over the continent, unaffected by discontinuities in soils and precipitation dataset collected by individual countries. In contrast with the VHI, ALEXI is based on energy balance, so radiation, atmospheric and soil moisture controls are all considered in the interpretation of the LST signal. The TIR remote sensing data used in the Evaporative Stress Index (ESI) also provide information about non-precipitation related moisture inputs to the land-surface system arising from processes such as irrigation, shallow groundwater sources, and lateral flows – processes that must be known a priori and modeled explicitly in prognostic LSMs (such as in NLDAS) but may significantly mitigate drought impacts during local rainfall deficits. And whereas vegetation index (VI) is a relatively slow response variable to moisture deficits, showing decline only after the damage has been done, thermal remote sensing has the potential to provide valuable drought early warning preceding detectable degradation in VIs.

## 2. Model methodology

The ALEXI surface energy balance model (Anderson *et al.* 1997, 2007a; Fig. 1) was specifically designed to minimize the need for ancillary meteorological data while maintaining a physically realistic representation of land-atmosphere exchange over a wide range in vegetation cover conditions. It is one of few land-surface models designed explicitly to exploit the high temporal resolution afforded by geostationary satellites.

### a. Interpretation of the thermal land-surface signature

Surface energy balance models estimate ET by partitioning the energy available at the land surface ( $RN - G$ , where  $RN$  is net radiation and  $G$  is the soil heat conduction flux, in  $\text{Wm}^{-2}$ ) into turbulent fluxes of sensible and latent heating ( $H$  and  $\lambda E$ , respectively,  $\text{Wm}^{-2}$ ):

$$RN - G = H + \lambda E \quad (1)$$

where  $\lambda$  is the latent heat of vaporization ( $\text{J kg}^{-1}$ ) and  $E$  is ET ( $\text{kg s}^{-1} \text{m}^{-2}$  or  $\text{mm s}^{-1}$ ). The land-surface representation in ALEXI model is based on the series version of the two-source energy balance (TSEB) model of Norman *et al.* (1995), which partitions the composite surface radiometric temperature,  $T_{RAD}$ , into characteristic soil and canopy temperatures,  $T_S$  and  $T_C$ , based on the local vegetation cover fraction apparent at the thermal sensor view angle,  $f(\theta)$ :

$$T_{RAD} \approx \{ f(\theta)T_c + [1 - f(\theta)] T_s \} \quad (2)$$

(Fig. 1), where  $f(\theta)$  can be related to leaf area index (LAI) using Beer's law. Eq. 2 is a linear approximation to an aggregation of surface radiance values. With information about  $T_{RAD}$ , LAI, and radiative forcing, the TSEB evaluates the soil (subscript 's') and the canopy ('c') energy budgets separately, computing system and component fluxes of net radiation ( $RN = RN_C + RN_S$ ), sensible and latent heat ( $H = H_C + H_S$  and  $\lambda E = \lambda E_C + \lambda E_S$ ), and soil heat ( $G$ ). Importantly, because angular effects are incorporated into the decomposition of  $T_{RAD}$ , the TSEB can accommodate TIR data acquired at off-nadir viewing angles by geostationary satellites. The TSEB has a built-in mechanism for detecting thermal signatures of stress in the soil and canopy. An initial iteration assumes the canopy transpiration ( $\lambda E_C$ ) is occurring at a potential (non-moisture limited) rate, while the soil evaporation rate ( $\lambda E_S$ ) is computed as a residual to the system energy budget. If the vegetation is stressed and transpiring at significantly less than the potential rate,  $\lambda E_C$  will be overestimated and the residual  $\lambda E_S$  will become negative. Condensation onto the soil is unlikely midday on clear days, and therefore  $\lambda E_S < 0$  is considered a signature of system stress. Under such circumstances, the  $\lambda E_C$  is iteratively down-regulated until  $\lambda E_S \sim 0$  (expected under dry conditions).

### b. ALEXI Evaporative Stress Index

The Evaporative Stress Index (Anderson *et al.* 2007 a, b; 2011) represents standardized anomalies in the ratio of actual-to-potential ET,  $f_{PET} = ET/PET$ , where ET and PET are instantaneous clear-sky estimates at shortly before local noon, retrieved using the ALEXI algorithm. Normalization by PET serves to minimize variability in ET due to seasonal variations in available energy and vegetation cover, further refining focus on the soil moisture signal. Limiting the assessment to clear-sky conditions separates signals of soil moisture

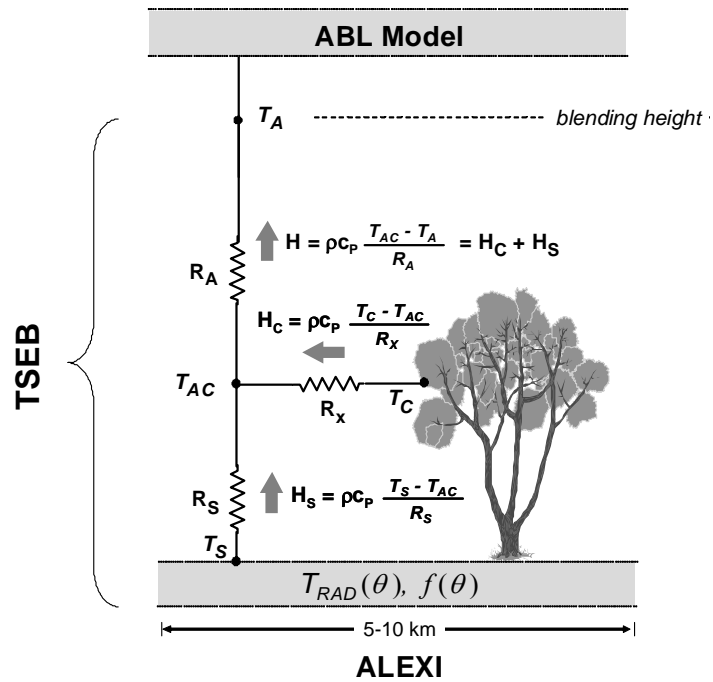


**Fig. 1** Schematic diagram representing the ALEXI modeling framework, highlighting fluxes of sensible heat ( $H$ ) from the soil and canopy (subscripts 's' and 'c') along gradients in temperature ( $T$ ), and regulated by transport resistances  $R_A$  (aerodynamic),  $R_x$  (bulk leaf boundary layer) and  $R_S$  (soil surface boundary layer).

variability from that of cloud climatology. To highlight differences in moisture conditions between years, standardized anomalies in  $f_{PET}$  are expressed as a pseudo z-score, normalized to a mean of zero and a standard deviation of one with respect to baseline fields describing “normal” (mean) conditions over the period of record.

### c. Model archive generation

Input datasets required by ALEXI are listed in Table 1. The sources of input data are a mix of operational inputs that are available daily (GOES Sounder / insolation and North American Regional Reanalysis (NARR) model output), and MODIS land products (such as LAI and albedo), which are routinely generated but available with a several week time lag. The ALEXI domain covers the CONUS at a spatial resolution of 10 km and a temporal resolution of 1 day.

Data	Purpose	Source	Spatial Resolution	Temporal Resolution
LST	$\Delta T_{rad}$ , RN	GOES	10 km	1 hr
LAI	$T_{rad}$ partitioning	MODIS	0.01°	8-day
Insolation	RN	GOES	20 km	1 hr
Longwave radiation	RN	GOES	20 km	1 hr
Albedo	RN	MODIS	0.05°	16-day
Wind Speed	Aerodynamic resistances	NARR	32 km	3 hr
Atmos lapse [dθ/dz]	ABL growth model	NARR	32 km	3 hr
Landcover type	Canopy characteristics	UMD	0.01	fixed

**Table 1** Primary inputs used by the current CONUS ALEXI ESI system.

## 3. Results

An intercomparison study of ALEXI ESI and a suite of drought indices (Table 2) was conducted from 2000 to 2011 over the CONUS, focusing on the primary growing season for most of the United States (April – October). As is the case with ESI, standardized anomalies were computed for each drought index. Temporal and spatial correlations between index anomalies were examined to assess the similarity between drought indices in their ability to rank drought severity and to visualize spatial patterns in index congruity.

Index	Acronym	Type
U.S. Drought Monitor	USDM	Multi-index synthesis
Evaporative Stress Index (X-month composite)	ESI-X	Remote sensing of $f_{PET}$
Vegetation Health Index	VHI	Remote sensing of LST, VI
Standardized precipitation index (X-month composite)	SPI-X	Precipitation
Palmer Z Index	Z	Precipitation + storage
Palmer drought severity index	PDSI	Precipitation + storage
Palmer modified drought index	PMDI	Precipitation + storage
Palmer hydrologic drought index	PHDI	Precipitation + storage
Noah-LDAS evapotranspiration	Noah-ET	Land surface model
Noah-LDAS soil moisture	Noah-SM	Land surface model

**Table 2** Drought indices included in the intercomparison study.

Drought features in the USDM classifications are generally reflected in one or more of the other indices but to varying degrees depending on drought type and time scale. Figure 2 shows the seasonal anomalies for a selection of drought indices listed in Table 2 for the study period of 2000 to 2011. In general, ESI reproduces patterns evident in the precipitation-based indices, indicating the value of the LST signal as a surface moisture proxy. For example, the thermal band inputs to ALEXI capture the major drought events in 2002 and 2007, even in the eastern United States, an area in which dense vegetation is dominant during the warm season. This is particularly important because standard soil moisture retrievals based on microwave remote sensing tend to lose sensitivity due to strong attenuation of the surface soil moisture signal by the overlying vegetative canopy. However, in this case, the thermal signal is able to detect vegetation stress related to root zone soil moisture deficits and elevated canopy temperatures.

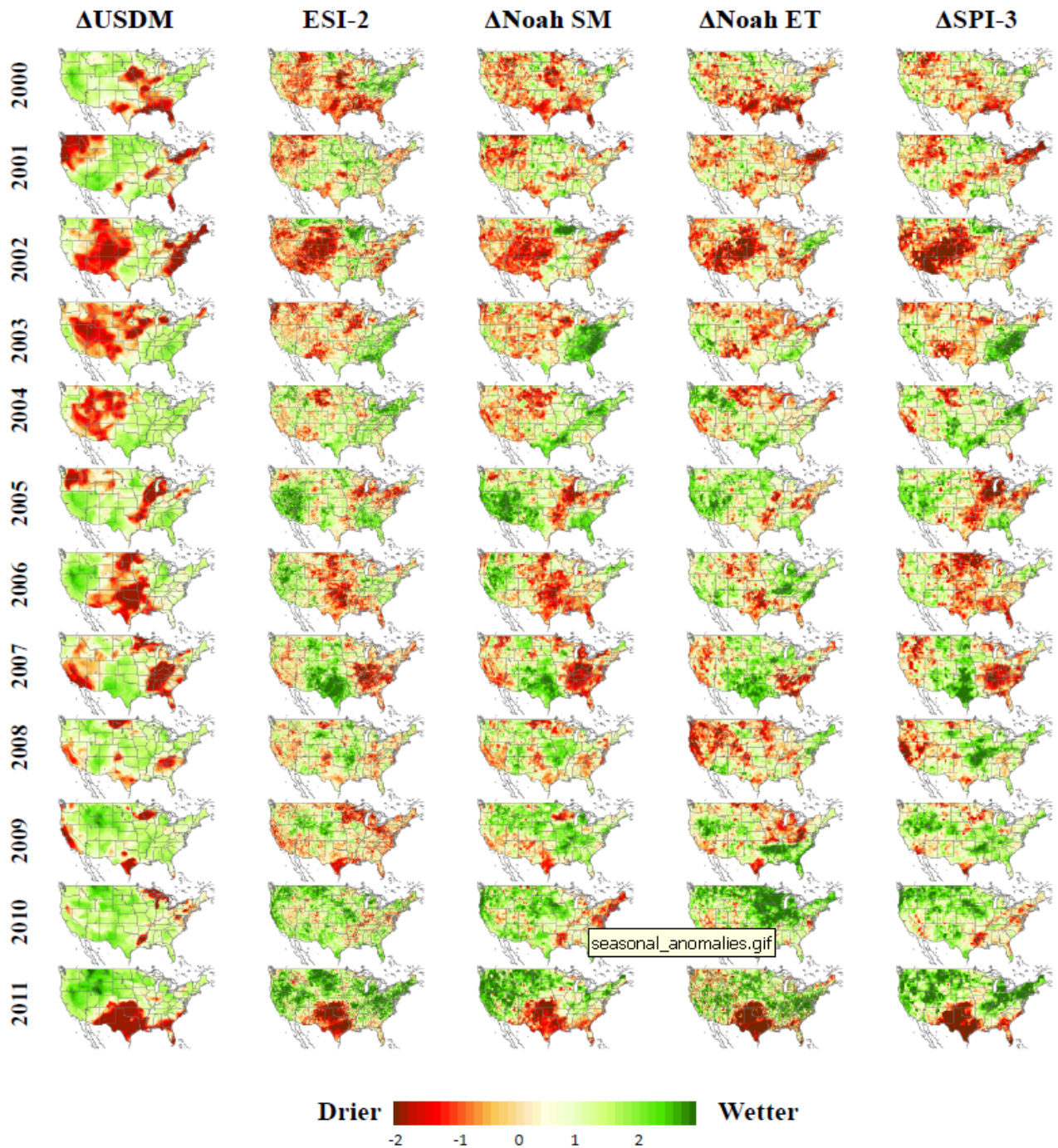


**Fig. 2** Seasonal (Apr-Oct) anomalies in US Drought Monitor classes, ESI, Noah soil moisture, Noah evapotranspiration and SPI-3.

Of the products included in the intercomparison, Noah soil moisture anomalies were found to be the most similar to the USDM with respect to temporal correlation (averaged over CONUS). The ALEXI 2-month ESI composite (ESI-2) shows higher average temporal correlations with the USDM than do the precipitation indices of shorter or comparable time scales (Z and SPI-1 to SPI-3). ESI-2 also outperforms Noah ET anomalies and VHI in terms of correlation with USDM. The strongest correlations between ESI and USDM are observed over the Great Plains and in the southeastern United States. These are areas identified by Karnieli *et al.* (2010) where LST and NDVI tend to be anticorrelated, indicating moisture-limiting (as opposed to energy limiting) vegetation growth conditions. In these areas, ET will be most sensitive to

changing root-zone soil moisture condition, and subsequently providing indications of drought. There are also regions where ESI shows reduced correlations with the USDM, e.g. over the Mississippi River basin, where shallow water tables and intensive irrigation tend to decouple ET rates from precipitation to some extent. ESI also shows lower correlations with the USDM over the Everglades in southern Florida, an area which is largely inundated with water over much of the year, and ET variations at the seasonal scale may be more related to climatic variability than to moisture availability. Finally, lower correlations are also found in the northern states where, particularly in early spring, ET is driven more by radiation and climate and is less tightly coupled with moisture conditions.

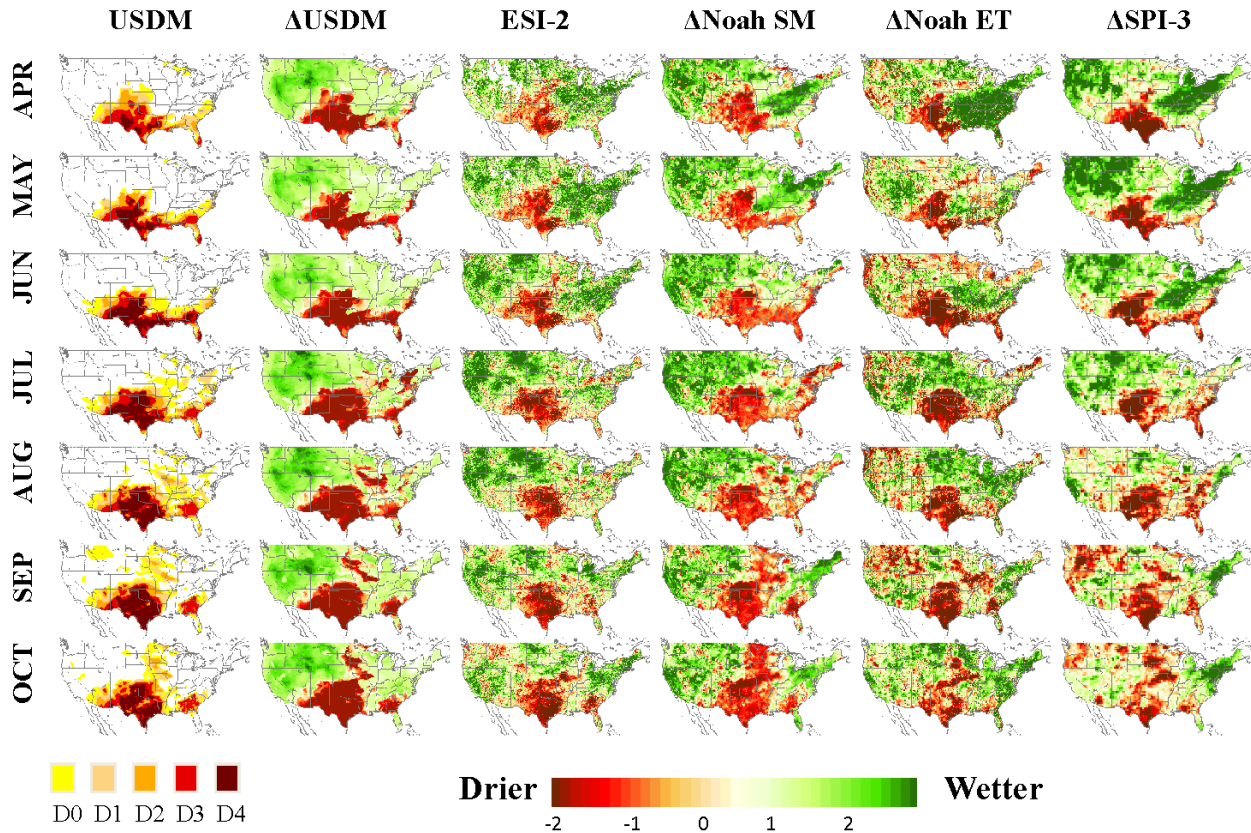


**Fig. 3** Monthly USDM drought classification and anomalies in USDM, ESI-2 Noah soil moisture, Noah evapotranspiration, and SPI-3 for 2011.

Spatial anomaly correlations were also computed to assess how well the indices agree on a spatial rather than temporal scale. On a seasonal (April–October) time-scale, all indices show the weakest correlations in 2003 during the long-term hydrologic drought event in the western CONUS, which is captured only by indices with time constants exceeding one year. The highest correlations, among all indices, is found during 2007 where there was a strong contrast in moisture conditions, with extensive drought conditions across the southeast US and anomalously wet conditions in the south central US. At the monthly time-scale, correlations between ESI-2 and the USDM are the weakest during April and May, likely due to poor temporal sampling in the ESI related to increased snow and cloud cover. However, spatial correlation with ESI-2 increases throughout the warm season as ET becomes more closely coupled to moisture conditions.

In contrast, correlations between the short-term precipitation indices ( $Z$ , SPI-2, SPI-3) and the USDM tend to degrade in August and September. An example of the monthly comparison of spatial anomalies between the USDM and ESI-2 is shown in Figure 3 for the year 2011. All five drought indices show excellent agreement with the extent and severity of the drought conditions across much of the south central US. However, an area of disagreement between ESI-2 and the USDM is evident in southern GA, where the USDM shows more severe drought conditions than is shown in ESI-2 during the period from May to August. ESI-2 does show small areas of dry conditions in May and June, yet conditions return to near normal during

July and August, before a rapid expansion of dry conditions in September through October. The improvement shown in July may be related to several precipitation events which likely lead to a replenishment of root-zone soil moisture and a decrease in vegetation stress. This is to some extent shown in both Noah SM and ET anomalies which showed slight improvement in July and August, although both Noah indices still had stronger negative anomalies than ESI-2 during both months. However, as dry conditions returned in August, root-zone soil moisture deficits likely increased and lead to a rapid appearance of significant dry anomalies in ESI-2 as shown in September and October.

A few caveats must be considered in this case, first, the USDM is not independent of many of the indices listed in Table 2, as they are commonly used in the construction of USDM drought classifications. ALEXI ESI was not used in the USDM classification process during the period of record in this analysis, and therefore is wholly independent. Second, the USDM drought classes incorporate information relevant to different kinds of drought over varying timescales, and we cannot expect a single indicator to agree perfectly with the USDM. For example, socioeconomic drought features in the USDM may indicate increased human demand for water rather than natural hydrological deficits. A more detailed analysis of all the drought index intercomparison results can be found in Anderson *et al.* (2011).

#### 4. Future Work

The final year of our NOAA-CPO project will mainly focus on two core objectives: (1) developing an open interface with end-users at the Climate Prediction Center (CPC) and the National Drought Mitigation Center (NDMC) to provide feedback on the use of ESI maps and (2) automating the ALEXI ESI system to provide weekly ESI maps to the National Integrated Drought Information System (NIDIS) portal and end-users at CPC and NDMC. Figure 4 shows an example of the ALEXI ESI website developed to provide ESI maps to end-users at CPC and NDMC. The website will be open to the entire drought community during the spring of 2012 and through the NIDIS portal at ([www.drought.gov](http://www.drought.gov)).

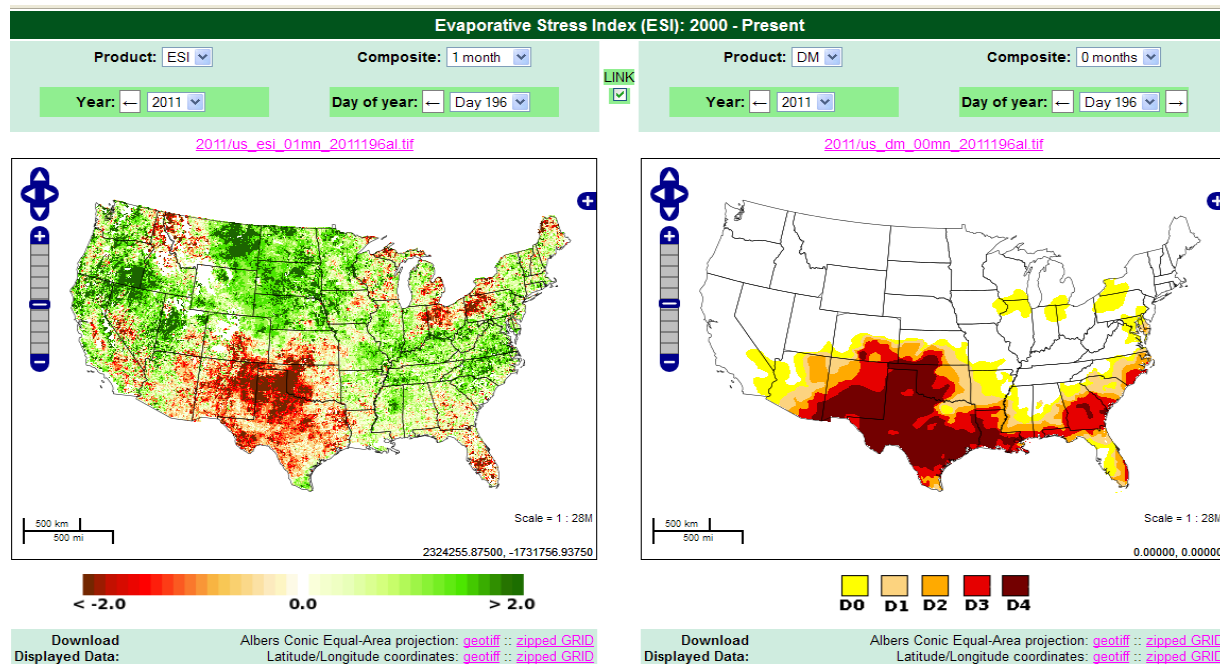


**Fig. 4** Screenshot of the ALEXI Evaporative Stress Index (ESI) website developed at the USDA Hydrology and Remote Sensing Lab.

Furthermore, the use of ALEXI as a proxy for soil moisture conditions will be expanded to produce an operational data assimilation system for the optimal assimilation of thermal and microwave soil moisture into the Noah LSM component of the NLDAS towards the goal of improved LSM-based drought monitoring. As mentioned earlier, ALEXI has been shown to perform well over densely vegetation regions such as the southeast US, an area in which microwave retrievals can suffer from significant vegetation-related errors.

Therefore, thermal and microwave retrievals methods have been shown to be quite complementary: thermal methods provide soil moisture information over a wide range of vegetation conditions, while microwave methods provide high temporal information (can retrieve through cloud cover) over areas of low vegetation cover (Hain *et al.* 2001). Finally, although this application of ESI focused solely on the CONUS, ALEXI domains are currently being developed both on a global scale (spatial resolution of 0.25°) and on a regional scale (*e.g.*, Europe, Africa, and Australia; spatial resolution of 3 to 10 km), facilitating production of ESI maps over these domains in the near future.

## References

- Anderson, M. C., J. M. Norman, G. R. Diak, W. P. Kustas, and J. R. Mecikalski, 1997: A two-source time-integrated model for estimating surface fluxes using thermal infrared remote sensing. *Remote Sens. Environ.*, **60**, 195-216.
- Anderson, M. C., J. M. Norman, J. R. Mecikalski, J. P. Otkin, and W. P. Kustas, 2007a: A climatological study of evapotranspiration and moisture stress across the continental U.S. based on thermal remote sensing: I. Model formulation. *J. Geophys. Res.*, **112**, D10117, doi:10.1029/2006JD007506.
- Anderson, M. C., J. M. Norman, J. R. Mecikalski, J. P. Otkin, and W. P. Kustas, 2007b: A climatological study of evapotranspiration and moisture stress across the continental U.S. based on thermal remote sensing: II. Surface moisture climatology. *J. Geophys. Res.*, **112**, D11112, doi:10.1029/2006JD007507.
- Anderson, M. C., C. R. Hain, B. D. Wardlow, A. Pimstein, J. R. Mecikalski and W. P. Kustas, 2011: Evaluation of drought indices based on thermal remote sensing of evapotranspiration over the continental United States. *J. of Climate*, **24**, 2025-2044.
- Brown, J. M., B. D. Wardlow, T. Tadesse, M. J. Hayes and B. C. Reed, 2008: The vegetation drought response index (VegDRI): A new integrated approach for monitoring drought stress in vegetation. *GIScience Remote Sens.*, **45**, 16-46.
- Hain, C. R., W. T. Crow, J. R. Mecikalski, M. C. Anderson, and T. Holmes (2011), An intercomparison of available soil moisture estimates from thermal infrared and passive microwave remote sensing and land surface modeling. *J. Geophys. Res.*, **116**, D15107, doi:10.1029/2011JD015633.
- Karnieli, A., N. Agam, R. T. Pinker, M. C. Anderson, M. L. Imhoff, G. G. Gutman, N. Panov, and A. Goldberg, 2010: Use of NDVI and LST for assessing vegetation health: merits and limitations. *J. Climate*, **23**, 618-633.
- Karnieli, A., M. Bayasgalan, Y. Bayarjargal, N. Agam, S. Khudulmur, and C. J. Tucker, 2006: Comments on the use of the Vegetation Health Index over Mongolia. *Int. J. Remote Sensing*, **27**, 2017-2024.
- Kogan, F. N., 1997: Global drought watch from space. *Bull. Amer. Meteorol. Soc.*, **78**, 621-636.
- McKee, T. B., N. J. Doesken, and J. Kleist, 1995: Drought monitoring with multiple time scales. Paper presented at AMS Ninth conf. on Applied Climatology, Dallas, TX.
- Mitchell, K. E. and Coauthors, 2003: The multi-institution North American Land Data Assimilation System (NLDAS): Utilizing multiple GCIP products and partners in a continental distributed hydrological modeling system. *J. Geophys. Res.*, **102**, doi:10.1029/2003JD002823.
- Norman, J. M., W. P. Kustas, and K. S. Humes, 1995: A two-source approach for estimating soil and vegetation energy fluxes from observations of directional radiometric surface temperature. *Agric. For. Meteorol.*, **77**, 263-293.
- Palmer, W.C., 1965: Meteorological drought. *Research Paper No. 45*, U.S. Weather Bureau, NOAA Library and Information Services Division, Washington, D.C. 20852, 58p.